Maximum-Likelihood Sequence Detector for Dynamic Mode High Density Probe Storage

Naveen Kumar, Pranav Agarwal, Aditya Ramamoorthy, and Murti V. Salapaka

***Abstract*—There is an increasing need for high density data storage devices driven by the increased demand of consumer electronics. In this work, we consider a data storage system that operates by encoding information as topographic profiles on a polymer medium. A cantilever probe with a sharp tip (few nm radius) is used to create and sense the presence of topographic profiles, resulting in a density of few Tb per in.^{2}. The prevalent mode of using the cantilever probe is the static mode that is harsh on the probe and the media. In this article, the high quality factor dynamic mode operation, that is less harsh on the media and the probe, is analyzed. The read operation is modeled as a communication channel which incorporates system memory due to inter-symbol interference and the cantilever state. We demonstrate an appropriate level of abstraction of this complex nanoscale system that obviates the need for an involved physical model. Next, a solution to the maximum likelihood sequence detection problem based on the Viterbi algorithm is devised. Experimental and simulation results demonstrate that the performance of this detector is several orders of magnitude better than the performance of other existing schemes.**

***Index Terms*—Nanotechnology, probe storage, maximum likelihood sequence detection, atomic force microscopy.**

I. Introduction

PRESENT day high density storage devices are primarily based on magnetic, optical and solid state technologies. Advanced signal processing and detection techniques have played an important role in the design of all data storage systems [1], [4], [10], [13]–[15], [24]. Indeed techniques such as partial-response max-likelihood [4], [21], [24] were responsible for significantly improving magnetic disk technology.

In this work, we consider a promising high density storage methodology which utilizes a sharp tip at the end of a micro cantilever probe to create, remove and read indentations (see [22]). The presence/absence of an indentation represents a bit of information. The main advantage of this method is the significantly higher areal densities compared to conventional technologies that are possible. Recently, experimentally achieved tip radii near 5 nm on a micro-cantilever were used to create areal densities close to 1 Tb/in^2 [22].

A particular realization of a probe based storage device that uses an array of cantilevers, along with the static mode operation is provided in [8]. However, there are fundamental drawbacks of this technique. In the static mode operation, the cantilever is in contact with media throughout the read operation which results in large vertical and lateral forces on the media and the tip. Moreover, significant information content is present in the low frequency region of the cantilever deflection and it can be shown experimentally that the system gain at low frequency is very small. Therefore, in order to overcome the measurement noise at the output, the interaction force between the tip and the medium has to be large. This degrades the medium and the probe over time, resulting in reduced device lifetime.

The problem of tip and media wear can be partly addressed by using the dynamic mode operation; particularly when a cantilever with a high quality factor is employed. In the dynamic mode operation, the cantilever is forced sinusoidally using a dither piezo. The oscillating cantilever gently taps the medium and thus the lateral forces are reduced which decreases the media wear [25]. Using cantilever probes that have high quality factors leads to high resolution, since the effect of a topographic change on the medium on the oscillating cantilever lasts much longer (approximately Q cantilever oscillation cycles, where each cycle is $1/f_0$ seconds long and Q and f_0 is the quality factor and the resonant frequency of the cantilever respectively). Moreover, the SNR improves as $\sqrt{Q}$ [23]. However, this also results in severe inter-symbol-interference, unless the topographic changes are spaced far apart. Spacing the changes far apart is undesirable from the storage viewpoint as it implies lower areal density. Another issue is that the cantilever exhibits complicated nonlinear dynamics. For example, if there is a sequence of hard hits on the media, then the next hit results in a milder response, i.e., the cantilever itself has inherent memory, that cannot be modeled as ISI. Conventional dynamic mode methods described in [17], that utilize high-Q cantilevers are not suitable for data storage applications. This is primarily because they are unable to deal with ISI and the nonlinear channel characteristics. The current techniques can be considered analogous to peak detection techniques in magnetic storage [14].

In this work we demonstrate that these issues can be addressed by modeling the dynamic mode operation as a communication system and developing high performance detectors for it. Note that corresponding activities have been undertaken in the past for technologies such as magnetic and optical storage [13], e.g., in magnetic storage, PRML techniques, resulted in tremendous improvements. In our work, the main issues are, (a) developing a model for the cantilever dynamics that predicts essential experimental features and remains tractable

Paper approved by H. Leib, the Editor for Communication and Information Theory of the IEEE Communications Society. Manuscript received April 12, 2009; revised August 30, 2009.

N. Kumar and A. Ramamoorthy are with the Dept. of Electrical and Computer Engg., Iowa State University, Ames IA 50011 (e-mail: {nk3, adityar}@iastate.edu).

P. Agarwal and M. V. Salapaka are with the Dept. of Electrical and Computer Engg., University of Minnesota, Minneapolis, MN 55455 (e-mail: {agar0108, murtis}@umn.edu).

This research was supported by NSF grant ECCS-0802019.

Digital Object Identifier 10.1109/TCOMM.2010.06.090197

for data storage purposes, and (b) designing high-performance detectors for this model, that allow the usage of high quality cantilevers, without sacrificing areal density. As discussed in the sequel, several concepts such as Markovian modeling of the cantilever dynamics and Viterbi detection in the presence of noise with memory [1], play a key role in our approach.

Main Contributions: In this article, a dynamic mode read operation is researched where the probe is oscillated and the media information is modulated on the cantilever probe's oscillations. It is demonstrated that an appropriate level of abstraction is possible that obviates the need for an involved physical model. The read operation is modeled as a communication channel which incorporates the system memory due to inter-symbol interference and the cantilever state that can be identified using training data. Using the identified model, a solution to the maximum likelihood sequence detection problem based on the Viterbi algorithm is devised. Experimental and simulation results which corroborate the analysis of the detector, demonstrate that the performance of this detector is several orders of magnitude better than the performance of other existing schemes and confirm performance gains that can render the dynamic mode operation feasible for high density data storage purposes.

Our work will motivate research for fabrication of prototypes that are massively parallel and employ high quality cantilevers (such as those used with the static mode [22] and intermittent contact dynamic mode but with low-Q [5]). In current prototypes, the cantilever detection is integrated into the cantilever structure and the cantilevers are actuated electrostatically. Even though the experimental setup reported in this article uses a particular scheme for measuring the cantilever detection and for actuating the cantilever, the paradigm developed for data detection is largely applicable in principle to other modes of detection and actuation of the cantilever. The analysis criteria primarily assume that high quality factor cantilevers are employed and that a dynamic mode operation is pursued.

The article is organized as follows. In Section II, background and related work of the probe based data storage system is presented. Section III deals with the problem of designing and analyzing the data storage unit as a communication system and finding efficient detectors for the channel model. Section IV and Section V report results from simulation and experiment respectively. Section VI provides the main findings of this article and future work.

II. Background and Related Work.

Probe based high density data storage devices employ a cantilever beam that is supported at one end and has a sharp tip at another end as a means to determine the topography of the media on which information is stored. The information on the media is encoded in terms of topographic profiles. A raised topographic profile is considered a high bit and a lowered topographic profile is considered a low bit. There are various means of measuring the cantilever deflection. In the standard atomic force microscope setup, which has formed the basis of probe based data storage, the cantilever deflection is measured by a beam-bounce method where a laser is incident on the back of the cantilever surface and the laser

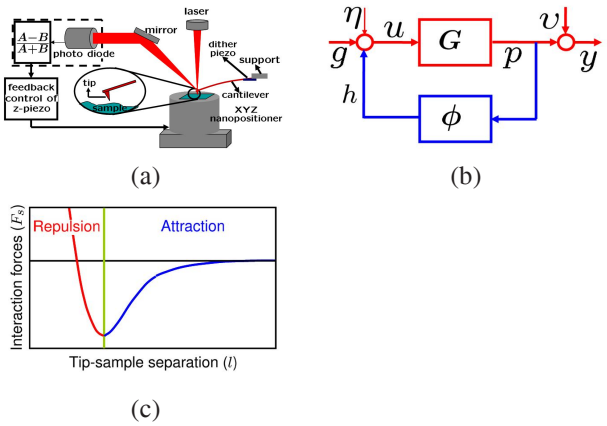

Fig. 1. (a) Shows the main components of a probe based storage device. The main probe is a cantilever with a tip at one end that interacts with the media. The support end can be forced using a dither piezo. The deflection of the tip-end is measured by a laser-mirror-photodiode arrangement. The controller employs the deflection measurement to keep the probe engaged with the media. (b) Shows a block diagram representation of the cantilever system G being forced by white noise (η), tip-media force h and the dither forcing g. The output of the block G, the deflection p is corrupted by measurement noise υ that results in the measurement y. Tip media force $h = \phi(p)$. (c) Shows the typical tip-media interaction forces of weak long range attractive forces and strong repulsive short range forces.

is reflected from the cantilever surface into a split photodiode. The photodiode collects the incident laser energy and provides a measure of the cantilever deflection (see Figure 1(a)). The advantage of the beam-bounce method is the high resolution (low measurement noise) and high bandwidth (in the 2-3 MHz) range. The disadvantage is that it cannot be easily integrated into an operation where multiple cantilevers operate in parallel. There are attractive measurement mechanisms that integrate the cantilever motion sensing onto the cantilever itself. These include piezo-resistive sensing [3] and thermal sensing [7]. For the dynamic mode operation there are various schemes to actuate the cantilever that include electrostatic [5], mechanical by means of a dither piezo that actuates the support of the cantilever base, magnetic [9] and piezoelectric [6]. In this article, it is assumed that the cantilever is actuated by a dither piezo and the sensing mechanism employed is the beam bounce method (see Figure 1(a)).

A. Models of cantilever probe, the measurement process and the tip-media interaction

A first mode approximation of the cantilever is given by the spring mass damper dynamics described by

$$\ddot{p} + \frac{\omega_0}{Q}\dot{p} + \omega_0^2 p = \mathfrak{f}(t), \;\; y = p + \upsilon, \tag{1}$$

where $\ddot{p} = \frac{d^2p}{dt^2}$, $p, \mathfrak{f}$, y and υ denote the deflection of the tip, the force on the cantilever, the measured deflection and the measurement noise respectively whereas the parameters ω_0 and Q are the first modal frequency (resonant frequency) and the quality factor of the cantilever respectively. The input-output transfer function with input $\mathfrak{f}$ and output p is given as $G = \frac{1}{s^2 + \frac{\omega_0}{Q}s + \omega_0^2}$. The cantilever model described above can be identified precisely (see [18]).

The interaction force, h, between the tip and the media depends on the deflection p of the cantilever tip. Such a

dependence is well characterized by the Lennard-Jones like force that is typically characterized by weak long-range attractive forces and strong short range repulsive forces (see Figure 1(c)). Thus, the probe based data storage system can be viewed as an interconnection of a linear cantilever system G with the nonlinear tip-media interaction forces in feedback (see Figure 1(b) and note that $p = G(h+\eta+g)$ with $h = \phi(p)$ [19]).

B. Cantilever-Observer Model

A state space representation of the filter G can be obtained as $\dot{\overline{x}} = A\overline{x} + B\mathfrak{f},\ y = C\overline{x} + \upsilon$ where $\overline{x} = [p\ \dot{p}]^T$ and $\mathfrak{f} = \eta + g$ (assuming no media forces h) and A, B and C are given by,

$$A = \begin{bmatrix} 0 & 1 \\ -\omega_0^2 & -\omega_0/Q \end{bmatrix},\quad B = \begin{bmatrix} 0 \\ 1 \end{bmatrix},\quad C = \begin{bmatrix} 1 & 0 \end{bmatrix}$$

Based on the model of the cantilever, an observer to monitor the state of the cantilever can be implemented [11] (see Figure 2). The observer dynamics and the associated state estimation error dynamics is given by,

$$\overbrace{\begin{aligned} \dot{\hat{\overline{x}}} &= A\hat{\overline{x}} + Bg + L(y - \hat{y}); \hat{\overline{x}}(0) = \hat{\overline{x}}_0, \\ \hat{y} &= C\hat{\overline{x}}, \end{aligned}}^{Observer}$$

$$\overbrace{\begin{aligned} \dot{\tilde{\overline{x}}} &= A\overline{x} + B(g+\eta) - A\hat{\overline{x}} - Bg - L(y - \hat{y}), \\ &= (A - LC)\tilde{\overline{x}} + B\eta - L\upsilon, \\ \tilde{\overline{x}}(0) &= \overline{x}(0) - \hat{\overline{x}}(0), \end{aligned}}^{State\ Estimation\ Error\ Dynamics}$$

where L is the gain of the observer, $\hat{\overline{x}}$ is the estimate of the state $\overline{x}$ and g is the external known dither forcing applied to the cantilever. The error in the estimate is given by $\tilde{\overline{x}} = \overline{x} - \hat{\overline{x}}$, whereas the error in the estimate of the output y is given by, $e = y - \hat{y} = C\tilde{\overline{x}} + \upsilon$. The error between the observed state and the actual state of the cantilever, when no noise terms or media forces are present ($\eta = \upsilon = h = 0$) is only due to the mismatch in the initial conditions of the observer and the cantilever-tip. Note that the cantilever tip interacts with the media only for a small portion of an oscillation. It is shown in [17] that such a tip-media interaction can be modeled well as an impact force (in other words as an impulsive force) on the cantilever that translates into an initial condition reset of the cantilever state. The error process is white if the Kalman gain is used for L [11]. For cantilever deflection sensors with low enough and realizable levels of measurement noise, the effective length of the impulse response of the system with media force as input and the error signal e as the output can be made as short as four periods of the cantilevers first resonant frequency.

As described in [17], the discretized model of the cantilever dynamics is given by

$$\begin{aligned} x_{k+1} &= Fx_k + G(g_k + \eta_k) + \delta_{\theta,k+1}\nu\ , \\ y_k &= Hx_k + v_k, k \geq 0\ , \end{aligned} \tag{2}$$

where the matrices F, G, and H are obtained from matrices A, B and C using the zero order hold discretization at a desired sampling frequency and $\delta_{i,j}$ denotes the dirac delta function. θ denotes the time instant when the impact between the cantilever tip and the media occurs and ν signifies the value of the impact. The impact results in an instantaneous change or jump in the state by ν at time instant θ. When a Kalman observer is used, the profile in the error signal due to the media can be pre-calculated as,

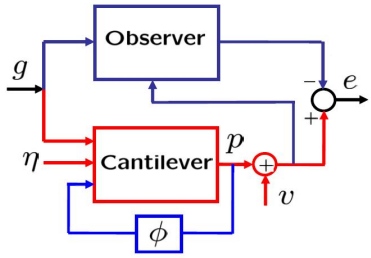

Fig. 2. An observer architecture for the system in Figure 1(b).

$$e_k = y_k - \hat{y}_k\ = \Gamma_{k;\theta}\ \nu + n_k\ , \tag{3}$$

where $\{\Gamma_{k;\theta}\ \nu\}$ is a known dynamic state profile with an unknown arrival time θ defined by $\Gamma_{k;\theta} = H(F - L_K H)^{k-\theta}$, for $k \geq \theta$. L_K is the Kalman observer gain, n_k is a zero mean white noise sequence which is the measurement residual had the impact not occurred and θ is assumed to be equal to 0 for simplicity. The statistics of n are given by, $E\{n_j n_k^T\} = V\delta_{jk}$ where $V = HP_{\tilde{\overline{x}}}H^T + R$ and $P_{\tilde{\overline{x}}}$ is the steady state error covariance obtained from the Kalman filter that depends on P and R which are the variances of the thermal noise and measurement noise respectively.

III. Channel Model and Detectors

A. Reformulation of state space representation

It is to be noted that although we have modeled the cantilever system as a spring-mass-damper model (second order system with no zeros and two stable poles)(see (1)), the experimentally identified channel transfer function that is more accurate in practice has right half plane zeros that are attributed to delays present in the electronics. Given this scenario, the state space representation used in [17] leads to a discrete channel with two inputs as seen in (3) because the structure of B is no longer in the form of $[0\ 1]^T$. However, source information enters the channel as a single input as the tip-medium interaction force. The problem can be reformulated as one of a channel being driven by a single input by choosing an appropriate state space representation. For the state space model of the cantilever, it is known that the pair (A, B) is controllable which implies there exists a transformation which will convert the state space into a controllable canonical form such that $B = [0\ 1]^T$. This kind of structure of B will force the discretized model (2) to be such that one component of ν is equal to 0. With B chosen as above, the entire system can be visualized as a channel that has a single source. In this article, the single source model is used as it simplifies the detector structure and analysis substantially.

B. Channel Model

The cantilever based data storage system can be modeled as a communication channel as shown in Figure 3. The components of this model are explained below in detail.

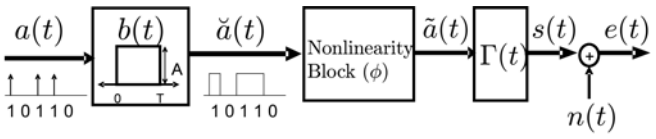

Fig. 3. Continuous time channel model of probe based data storage system.

Shaping Filter ($b(t)$): The model takes as input the bit sequence $\bar{a} = (a_0,\ a_1 \dots\ a_{N-1})$ where $a_k, k = 1, \dots, N-1$ is equally likely to be 0 or 1. In the probe storage context, '0' refers to the topographic profile being *low* and '1' refers to the topographic profile being *high*. Each bit has a duration of T seconds. This duration can be found based on the length of the topographic profile specifying a single bit and the speed of the scanner. The height of the high bit is denoted by A. The cantilever interacts with the media by gently tapping it when it is high. When the media is low, typically no interaction takes place. We model the effect of the medium height using a filter with impulse response $b(t)$ (shown in Figure 3) that takes as input, the input bit impulse train $a(t) = \sum_{k=0}^{N-1} a_k \delta(t - kT)$. The output of the filter is given by $\breve{a}(t) = \sum_{k=0}^{N-1} a_k b(t - kT)$.
Nonlinearity Block (ϕ): The cantilever oscillates at frequency f_0 which means that in each cantilever cycle of duration $T_c = 1/f_0$, the cantilever hits the media at most once if the media is high during a time T_c. Due to the dynamics of the system it may not hit the media, even if it is high. The magnitude of impact on the media is not constant and changes according to the state of the cantilever prior to the interaction with the media. We note that a very accurate modeling of the cantilever trajectory will require the solution of complex nonlinear equations corresponding to the cantilever dynamics and knowledge of the bit profile so that each interaction is known. In this work we model the impact values of the tip-media interaction by means of a probabilistic Markov model that depends on the previous bits. This obviates the need for a detailed model. We assume that in each high bit duration T, the cantilever hits the media q times (i.e. $T = qT_c$) with varying magnitudes. Therefore, for N bits, the output of the nonlinearity block is given by, $\tilde{a}(t) = \sum_{k=0}^{Nq-1} \nu_k(\bar{a}) \delta(t - kT_c)$, where ν_k denotes the magnitude of the k^{th} impact of the cantilever on the medium. Here, we approximate the nonlinearity block output as a sequence of impulsive force inputs to the cantilever. The strength of the impulsive hit at any instant is dependent on previous impulsive hits; precisely because the previous interactions affect the amplitude of the oscillations that in turn affect how hard the hit is at a particular instance. The exact dependence is very hard to model deterministically and therefore we chose a Markov model, as given below for the sequence of impact magnitudes for a single bit duration,

$$\bar{\nu}_i = \bar{\mathfrak{G}}(a_i, a_{i-1}, \dots, a_{i-m}) + \bar{\mathfrak{b}}_i \tag{4}$$

where $\bar{\mathfrak{G}}(a_i, a_{i-1}, \dots, a_{i-m})$ is a function of the current and the last m bits and $\bar{\nu}_i = [\nu_{iq}\ \nu_{iq+1} \dots \nu_{(i+1)q-1}]^T$. Here m denotes the system memory and $\bar{\mathfrak{b}}_i$ is a zero mean i.i.d. Gaussian vector of length q. The appropriateness of the model will be demonstrated by our experimental results.
Channel Response ($\Gamma(t)$): The Markovian modeling of the output of the nonlinearity block as discussed above allows us to break the feedback loop in Figure 2 (see also [17]). The rest of the system can then be modeled by treating it as a linear system with impulse response $\Gamma(t)$. $\Gamma(t)$ is the error between the cantilever tip deflection and the tip deflection as estimated by the observer when the cantilever tip is subjected to an impulsive force. It can be found in closed form for a given set of parameters of cantilever-observer system (see (3)).
Channel Noise ($n(t)$): The measurement noise (from the imprecision in measuring the cantilever position) and thermal noise (from modeling mismatches) can be modeled by a single zero mean white Gaussian noise process ($n(t)$) with power spectral density equal to V.

The continuous time innovation output $e(t)$ becomes, $e(t) = s(t, \bar{\nu}(\bar{a})) + n(t)$, where $s(t, \bar{\nu}(\bar{a})) = \sum_{k=0}^{Nq-1} \nu_k(\bar{a}) \Gamma(t - kT_c)$ and $\bar{\nu}(\bar{a}) = (\nu_0(\bar{a}),\ \nu_1(\bar{a}) \dots\ \nu_{Nq-1}(\bar{a}))$. The sequence of impact values $\bar{\nu}_i$ is assumed to follow a Markovian model as explained above, $\Gamma(t)$ is the channel impulse response and $n(t)$ is a zero mean white Gaussian noise process.

C. Sufficient Statistics for Channel model

Before providing sufficient statistics we consolidate the notation used. The source stream is N elements long ($\bar{a}$ denotes the sequence of source bits), with the topographic profile and the scan speed is chosen such that the cantilever impacts any topographic profile q times. Thus there are Nq possible hits with $\bar{\nu}(\bar{a})$ denoting the sequence of strength of the Nq impulsive hits on the cantilever. Furthermore, the set of strengths of impulsive force inputs, which is q elements long, during the i^{th} topographic profile encoding the i^{th} source symbol is denoted by $\bar{\nu}_i$. Given the probabilistic model on $\bar{\nu}$ and finite bit sequence ($\bar{a}$), an information lossless decomposition of $e(t)$ by expansion over an orthonormal finite-dimensional basis with dimension $\tilde{N}$ can be achieved where $\tilde{N}$ orthonormal basis functions span the signal space formed by $s(t, \bar{\nu}(\bar{a}))$. The components of $e(t)$ over $\tilde{N}$ orthonormal basis functions are given by, $\bar{\mathfrak{e}} = \bar{s}(\bar{\nu}(\bar{a})) + \bar{n}$, where $\bar{\mathfrak{e}} = (\mathfrak{e}_0,\ \mathfrak{e}_1 \dots\ \mathfrak{e}_{\tilde{N}})$, $\bar{s}(\bar{\nu}(\bar{a})) = (s_0,\ s_1 \dots\ s_{\tilde{N}})$, $\bar{n} = (n_0,\ n_1 \dots\ n_{\tilde{N}})$ and $\bar{n} \sim N(0, VI_{\tilde{N} \times \tilde{N}})$ where $I_{\tilde{N} \times \tilde{N}}$ stands for $\tilde{N} \times \tilde{N}$ identity matrix [10]. The maximum likelihood estimate of the bit sequence can be found as $\hat{\bar{a}} = \arg\max_{\bar{a} \in \{0,1\}^N} f(\bar{\mathfrak{e}}|\bar{a})$ where $\hat{\bar{a}} = (\hat{a}_0,\ \hat{a}_1 \dots \hat{a}_{N-1})$ is the estimated bit sequence and f denotes a pdf. The term $f(\bar{\mathfrak{e}}|\bar{a})$ can be further simplified as,

$$f(\bar{\mathfrak{e}}|\bar{a}) = \int_{\bar{\nu}} f(\bar{\mathfrak{e}}|\bar{a}, \bar{\nu}) f(\bar{\nu}|\bar{a}) d\bar{\nu} = \int_{\bar{\nu}} \frac{1}{(2\pi V)^{\frac{\tilde{N}}{2}}} \times \exp \frac{-||\bar{\mathfrak{e}} - \bar{s}(\bar{\nu}(\bar{a}))||^2}{2V} f(\bar{\nu}|\bar{a}) d\bar{\nu} = \frac{1}{(2\pi V)^{\frac{\tilde{N}}{2}}} \exp \frac{-||\bar{\mathfrak{e}}||^2}{2V} \times \int_{\bar{\nu}} \exp \frac{-(||\bar{s}(\bar{\nu}(\bar{a}))||^2 - 2\bar{\mathfrak{e}}^T \bar{s}(\bar{\nu}(\bar{a})))}{2V} f(\bar{\nu}|\bar{a}) d\bar{\nu}$$

where $||.||^2$ denotes Euclidean norm, $f(\bar{\mathfrak{e}}|\bar{a}, \bar{\nu})$ and $f(\bar{\nu}|\bar{a})$ denote the respective conditional pdf's and $\bar{\nu} = (\nu_0,\ \nu_1 \dots\ \nu_{Nq-1})$. The correlation between $\bar{\mathfrak{e}}$ and $\bar{s}(\bar{\nu}(\bar{a}))$ can be equivalently expressed as an integral over time because of the orthogonal decomposition procedure ,i.e., $\bar{\mathfrak{e}}^T \bar{s}(\bar{\nu}(\bar{a})) = \int_{-\infty}^{\infty} e(t) s(t, \bar{\nu}(\bar{a})) dt = \bar{\nu}^T \bar{z}'$, where $\bar{\nu} = (\nu_0,\ \nu_1 \dots\ \nu_{Nq-1})$, $\bar{z}' = (z'_0,\ z'_1 \dots\ z'_{Nq-1})$ and $z'_k = \int_{-\infty}^{\infty} e(t) \Gamma(t - kT_c) dt$ for $0 \le k \le Nq - 1$ is the output

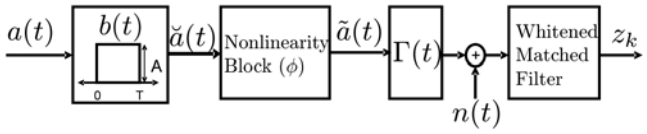

Fig. 4. Discretized channel model with whitened matched filter.

of a matched filter $\Gamma(-t)$ with input $e(t)$ sampled at $t = kT_c$. The term $f(\bar{\mathfrak{e}}|\bar{a})$ can now be written as,

$$f(\bar{\mathfrak{e}}|\bar{a}) = \underbrace{\frac{1}{(2\pi V)^{\frac{N}{2}}} \exp \frac{-||\bar{\mathfrak{e}}||^2}{2V}}_{\mathfrak{h}(\bar{\mathfrak{e}})} \times \underbrace{\int_{\bar{\nu}} \exp \frac{-||\bar{s}(\bar{\nu}(\bar{a}))||^2}{2V} \exp \frac{\bar{\nu}^T \bar{z}'}{V} f(\bar{\nu}|\bar{a}) d\bar{\nu}}_{\mathfrak{F}(\bar{z}'|\bar{a})}$$

So $f(\bar{\mathfrak{e}}|\bar{a})$ can be factorized into $\mathfrak{h}(\bar{\mathfrak{e}})$ (dependent only on $\bar{\mathfrak{e}}$) and $\mathfrak{F}(\bar{z'}|\bar{a})$ (for a given $\bar{a}$ dependent only on $\bar{z'}$). Using the Fisher-Neyman factorization theorem [2], we can claim that $\bar{z'}$ is a vector of sufficient statistics for the detection process i.e. $\frac{f(\bar{e}|\bar{a})}{f(\bar{z'}|\bar{a})} = \mathcal{C}$, where $\mathcal{C}$ is a constant independent of $\bar{a}$. So we can reformulate the detection problem as, $\hat{\bar{a}} = \arg\max_{\bar{a}\in\{0,1\}^N} f(\bar{z'}|\bar{a})$ which means that bit detection problem depends only on the matched filter outputs ($\bar{z'}$). These matched filter outputs for $0 \le k \le Nq-1$ can be further simplified as, $z'_k = \sum_{k_1=0}^{Nq-1} \nu_{k_1}(\bar{a}) h'_{k-k_1} + n'_k$, where $h'_{k-k_1} = \int_{-\infty}^{\infty} \Gamma(t-kT_c)\Gamma(t-k_1T_c)dt$ and $n'_k = \int_{-\infty}^{\infty} n(t)\Gamma(t-kT_c)dt$ such that $E(n'_k n'_{k'}) = \int_{-\infty}^{\infty}\int_{-\infty}^{\infty} E(n(t)n(\tau))\Gamma(t-kT_c)\Gamma(\tau-k'T_c)dtd\tau = VR_{k-k'}$, where $R_{k-k'} = \int_{-\infty}^{\infty}\Gamma(t-kT_c)\Gamma(t-k'T_c)dt$. A whitening matched filter can be determined to whiten output noise n'_k [10]. We shall denote the discretized output of whitened matched filter shown in Figure 4 as z_k, such that $z_k = \sum_{k_1=0}^{I} \nu_{k-k_1}(\bar{a}) h_{k_1} + n_k$, where the filter $\{h_k\}_{k=0,1,\ldots,I}$ denotes the effect of the whitened matched filter and the sequence $\{n_k\}$ represents the Gaussian noise with variance V.

D. Viterbi Detector Design

Note that the outputs of the whitened matched filter $\bar{z}$, continue to remain sufficient statistics for the detection problem. Therefore, we can reformulate the detection strategy as,

$$\begin{aligned}\hat{\bar{a}} &= \arg\max_{\bar{a}\in\{0,1\}^N} f(\bar{z}|\bar{a}) \\ &= \arg\max_{\bar{a}\in\{0,1\}^N} \Pi_{i=0}^{N-1} f(\bar{z}_i|\bar{a}, \bar{z}_0^{i-1}) \end{aligned} \quad (5)$$

where $\bar{z} = [z_0 \ z_1 \ldots z_{Nq-1}]^T$, $\bar{z}_i$ is the received output vector corresponding to the i^{th} input bit, i.e., $\bar{z}_i = [z_{iq} \ z_{iq+1} \ldots z_{(i+1)q-1}]^T$ and $\bar{z}_0^{i-1} = [\bar{z}_0^T \ \bar{z}_1^T \ldots \bar{z}_{i-1}^T]^T$. In our model, the channel is characterized by finite impulse response of length I i.e. $h_i = 0$ for $i < 0$ and $i > I$ and we assume that $I \le m_I q$ i.e. the inter-symbol-interference (ISI) length in terms of q hits is equal to m_I. Let m be the system memory (see (4)). The length of channel response is known which means that m_I is known but the value of m cannot be found because it depends on the experimental parameters of the system. In the experimental results section, we describe how we find the value of m from experimental data. The received output vector $\bar{z}_i$ can now be written as,

$$\begin{aligned}\bar{z}_i &= \begin{pmatrix} h_I & . & . & h_0 & 0 & . & . & 0 \\ 0 & h_I & . & . & h_0 & 0 & . & 0 \\ . & . & . & . & . & . & . & . \\ 0 & . & . & 0 & h_I & . & . & h_0 \end{pmatrix} \begin{pmatrix} \nu_{iq-I} \\ \nu_{1+iq-I} \\ \vdots \\ \nu_{(i+1)q-1} \end{pmatrix} + \bar{n}_i \\ &= H\bar{\nu}_{i-m_I}^i + \bar{n}_i, \end{aligned}$$

where $\bar{\nu}_i = [\nu_{iq} \ \nu_{iq+1} \ldots \nu_{(i+1)q-1}]^T$, $\bar{\nu}_{i-m_I}^i = [\bar{\nu}_{i-m_I}^T \ \ldots \ \bar{\nu}_i^T]^T$ and $\bar{n}_i = [n_{iq} \ n_{1+iq} \ldots n_{(i+1)q-1}]^T$.

Our next task is to simplify the factorization in (5) so that decoding can be made tractable. We construct the dependency graph of the concerned quantities which is shown in Figure 5. Using the Bayes ball algorithm [20], we conclude that

$$f(\bar{z}_i|\bar{\nu}_{i-m_I}^i, \bar{a}, \bar{z}_0^{i-1}) = f(\bar{z}_i|\bar{\nu}_{i-m_I}^i), \quad (6)$$

$$f(\bar{\nu}_{i-m_I}|\bar{a}, \bar{z}_0^{i-1}) = f(\bar{\nu}_{i-m_I}|a_0^{i-1}, \bar{z}_0^{i-1}), \quad (7)$$

$$f(\bar{\nu}_{i-k}|\bar{\nu}_{i-m_I}^{i-k-1}, \bar{a}, \bar{z}_0^{i-1}) = f(\bar{\nu}_{i-k}|\bar{\nu}_{i-m_I}^{i-k-1}, a_0^{i-m_I-1}, a_{i-m-k}^{i-1}, \bar{z}_0^{i-1}), \forall\ 1 \le k \le m_I - 1 \quad (8)$$

$$f(\bar{\nu}_i|\bar{\nu}_{i-m_I}^{i-1}, \bar{a}, \bar{z}_0^{i-1}) = f(\bar{\nu}_i|a_{i-m}^i) \quad (9)$$

where $a_0^{i-1} = [a_0 \ a_1 \ \ldots \ a_{i-1}]$. Although the conditional pdf $f(\bar{\nu}_{i-k}|\bar{\nu}_{i-m_I}^{i-k-1}, \bar{a}, \bar{z}_0^{i-1})$ and $f(\bar{\nu}_{i-m_I}|\bar{a}, \bar{z}_0^{i-1})$ depend on the entire past, we assume that these dependencies are rapidly decreasing with increase in past time. This is observed in simulation and experimental data as well. For making the detection process more tractable, we make the following assumptions on this dependence,

$$f(\bar{\nu}_{i-m_I}|a_0^{i-1}, \bar{z}_0^{i-1}) \approx f(\bar{\nu}_{i-m_I}|a_{i-m-m_I}^{i-1}, \bar{z}_{i-m_I}^{i-1}) \quad (10)$$

$$f(\bar{\nu}_{i-k}|\bar{\nu}_{i-m_I}^{i-k-1}, a_0^{i-m_I-1}, a_{i-m-k}^{i-1}, \bar{z}_0^{i-1}) \approx f(\bar{\nu}_{i-k}|\bar{\nu}_{i-m_I}^{i-k-1}, a_{i-k-m}^{i-1}, \bar{z}_{i-k}^{i-1}), \forall\ 1 \le k \le m_I - 1 \quad (11)$$

i.e. the dependence is restricted to only the immediate neighbors in the dependency graph. Using the above assumptions and dependency graph results, $f(\bar{z}_i|\bar{a}, \bar{z}_0^{i-1})$ can be further simplified as,

$$\begin{aligned} f(\bar{z}_i|\bar{a}, \bar{z}_0^{i-1}) &= \int f(\bar{z}_i|\bar{\nu}_{i-m_I}^i, \bar{a}, \bar{z}_0^{i-1}) f(\bar{\nu}_{i-m_I}^i|\bar{a}, \bar{z}_0^{i-1}) d\bar{\nu}_{i-m_I}^i \\ &= \int f(\bar{z}_i|\bar{\nu}_{i-m_I}^i, \bar{a}, \bar{z}_0^{i-1}) f(\bar{\nu}_{i-m_I}|\bar{a}, \bar{z}_0^{i-1}) \\ &\cdot \Pi_{k=1}^{m_I-1} f(\bar{\nu}_{i-k}|\bar{\nu}_{i-m_I}^{i-k-1}, \bar{a}, \bar{z}_0^{i-1}) f(\bar{\nu}_i|\bar{\nu}_{i-m_I}^{i-1}, \bar{a}, \bar{z}_0^{i-1}) d\bar{\nu}_{i-m_I}^i \\ &= \int f(\bar{z}_i|\bar{\nu}_{i-m_I}^i) f(\bar{\nu}_{i-m_I}|a_0^{i-1}, \bar{z}_0^{i-1}) \\ &\cdot \Pi_{k=1}^{m_I-1} f(\bar{\nu}_{i-k}|\bar{\nu}_{i-m_I}^{i-k-1}, a_0^{i-m_I-1}, a_{i-m-k}^{i-1}, \bar{z}_0^{i-1}) \\ &\cdot f(\bar{\nu}_i|a_{i-m}^i) d\bar{\nu}_{i-m_I}^i \text{(Using (6),(7),(8),(9))} \\ &= \int f(\bar{z}_i|\bar{\nu}_{i-m_I}^i) f(\bar{\nu}_{i-m_I}|a_{i-m-m_I}^{i-1}, \bar{z}_{i-m_I}^{i-1}) \\ &\cdot \Pi_{k=1}^{m_I-1} f(\bar{\nu}_{i-k}|\bar{\nu}_{i-m_I}^{i-k-1}, a_{i-k-m}^{i-1}, \bar{z}_{i-k}^{i-1}) \\ &\cdot f(\bar{\nu}_i|a_{i-m}^i) d\bar{\nu}_{i-m_I}^i \text{(Using (10),(11))} \\ &= f(\bar{z}_i|a_{i-m-m_I}^i, \bar{z}_{i-m_I}^{i-1}). \end{aligned}$$

By defining a state $S_i = a_{i-m-m_I+1}^i$, this can be further expressed as $f(\bar{z}_i|S_i, S_{i-1}, \bar{z}_{i-m_I}^{i-1})$. Again using Bayes ball algorithm, we conclude that

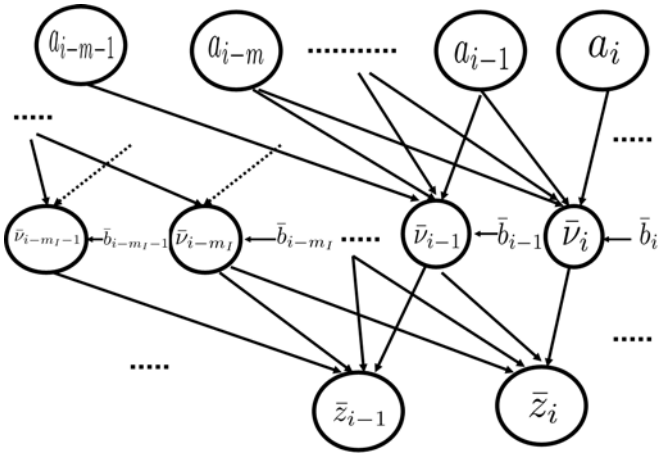

Fig. 5. Dependency graph for the model with $I = m_I q$ and m is the system memory of the system.

$$f(\bar{z}^i_{i-m_I}|\bar{\nu}^i_{i-2m_I}, a^i_{i-m-m_I}) = f(\bar{z}^i_{i-m_I}|\bar{\nu}^i_{i-2m_I}), \quad (12)$$

$$\Pi_{k=1}^{2m_I-1} f(\bar{\nu}_{i-2m_I+k}|\bar{\nu}^{i-2m_I+k-1}_{i-2m_I}, a^i_{i-m-m_I}) = \Pi_{k=1}^{m_I-1} f(\bar{\nu}_{i-2m_I+k}|\bar{\nu}^{i-2m_I+k-1}_{i-2m_I}, a^i_{i-m-m_I}) \cdot \Pi_{k=m_I}^{2m_I-1} f(\bar{\nu}_{i-2m_I+k}|a^{i-2m_I+k}_{i-2m_I-m+k}), \quad (13)$$

$$f(\bar{\nu}_i|\bar{\nu}^{i-1}_{i-2m_I}, a^i_{i-m-m_I}) = f(\bar{\nu}_i|a^i_{i-m}). \quad (14)$$

The pdf of $\bar{z}^i_{i-m_I} = [\bar{z}^T_{i-m_I} \ \dots \ \bar{z}^T_i]^T$ given current state S_i and previous state S_{i-1} is given by,

$$\begin{aligned} f(\bar{z}^i_{i-m_I}|S_i, S_{i-1}) &= f(\bar{z}^i_{i-m_I}|a^i_{i-m-m_I}) \\ &= \int f(\bar{z}^i_{i-m_I}|\bar{\nu}^i_{i-2m_I}, a^i_{i-m-m_I}) f(\bar{\nu}^i_{i-2m_I}|a^i_{i-m-m_I}) d\bar{\nu}^i_{i-2m_I} \\ &= \int f(\bar{z}^i_{i-m_I}|\bar{\nu}^i_{i-2m_I}, a^i_{i-m-m_I}) f(\bar{\nu}_{i-2m_I}|a^i_{i-m-m_I}) \\ &\cdot \Pi_{k=1}^{2m_I-1} f(\bar{\nu}_{i-2m_I+k}|\bar{\nu}^{i-2m_I+k-1}_{i-2m_I}, a^i_{i-m-m_I}) \\ &\cdot f(\bar{\nu}_i|\bar{\nu}^{i-1}_{i-2m_I}, a^i_{i-m-m_I}) d\bar{\nu}^i_{i-2m_I} \\ &= \int f(\bar{z}^i_{i-m_I}|\bar{\nu}^i_{i-2m_I}) f(\bar{\nu}_{i-2m_I}|a^i_{i-m-m_I}) \Pi_{k=1}^{m_I-1} \\ &\cdot f(\bar{\nu}_{i-2m_I+k}|\bar{\nu}^{i-2m_I+k-1}_{i-2m_I}, a^i_{i-m-m_I}) \Pi_{k=m_I}^{2m_I-1} f(\bar{\nu}_{i-2m_I+k}| \\ & a^{i-2m_I+k}_{i-2m_I-m+k}) f(\bar{\nu}_i|a^i_{i-m}) d\bar{\nu}^i_{i-2m_I} \text{(Using (12),(13),(14))} \end{aligned}$$

where the last step is obtained using results from dependency graph and all the terms in the last step except $f(\bar{\nu}_{i-2m_I}|a^i_{i-m-m_I})$ and $\Pi_{k=1}^{m_I-1} f(\bar{\nu}_{i-2m_I+k}|\bar{\nu}^{i-2m_I+k-1}_{i-2m_I}, a^i_{i-m-m_I})$ are Gaussian distributed. This implies that the pdf of $\bar{z}^i_{i-m_I}$ given (S_i, S_{i-1}) is not exactly Gaussian distributed. If the number of states in the detector is increased it can be modeled as a Gaussian which means that the term like $f(\bar{\nu}_{i-2m_I}|a^i_{i-m-m_I})$ can be made Gaussian distributed by increasing the number of states, but this increases the complexity. In order to keep the decoding tractable we make the assumption that $f(\bar{z}^i_{i-m_I}|S_i, S_{i-1})$ is Gaussian i.e. $f(\bar{z}^i_{i-m_I}|S_i, S_{i-1}) \sim N(\bar{\mathcal{Y}}(S_i, S_{i-1}), \mathcal{C}(S_i, S_{i-1}))$, where $\bar{\mathcal{Y}}(S_i, S_{i-1})$ is the mean and $\mathcal{C}(S_i, S_{i-1})$ is the covariance. With our state definition, we can reformulate the detection problem as a maximum likelihood state sequence detection problem [1],

$$\begin{aligned} \hat{\bar{S}} &= \arg\max_{all\ \bar{S}} \ f(\bar{z}|\bar{S}) = \arg\max_{all\ \bar{S}} \ \Pi_{i=0}^{N-1} \ f(\bar{z}_i|\bar{S}, \bar{z}_0 \dots \bar{z}_{i-1}) \\ &= \arg\max_{all\ \bar{S}} \ \Pi_{i=0}^{N-1} \ f(\bar{z}_i|S_i, S_{i-1}, \bar{z}^{i-1}_{i-m_I}) \\ &= \arg\max_{all\ \bar{S}} \ \Pi_{i=0}^{N-1} \frac{f(\bar{z}^i_{i-m_I}|S_i, S_{i-1})}{f(\bar{z}^{i-1}_{i-m_I}|S_i, S_{i-1})} \\ &= \arg\min_{all\ \bar{S}} \ \sum_{i=0}^{N-1} \log \frac{|\mathcal{C}(S_i, S_{i-1})|}{|c(S_i, S_{i-1})|} + (\bar{z}^i_{i-m_I} - \bar{\mathcal{Y}}(S_i, S_{i-1}))^T \\ &\cdot \mathcal{C}(S_i, S_{i-1})^{-1} (\bar{z}^i_{i-m_I} - \bar{\mathcal{Y}}(S_i, S_{i-1})) - (\bar{z}^{i-1}_{i-m_I} \\ &- \bar{\mathbf{y}}(S_i, S_{i-1}))^T c(S_i, S_{i-1})^{-1} (\bar{z}^{i-1}_{i-m_I} - \bar{\mathbf{y}}(S_i, S_{i-1})) \end{aligned}$$

where $\hat{\bar{S}}$ is estimated state sequence, $c(S_i, S_{i-1})$ is the upper $m_I q \times m_I q$ principal minor of $\mathcal{C}(S_i, S_{i-1})$ and $\bar{\mathbf{y}}(S_i, S_{i-1})$ collects the first $m_I q$ elements of $\bar{\mathcal{Y}}(S_i, S_{i-1})$. It is assumed that the first state is known. With metric given above, Viterbi decoding can be applied to get the maximum likelihood state sequence and the corresponding bit sequence.

E. LMP, GLRT and Bayes Detector

In [17], the hit detection algorithm is proposed which ignores the modeling of channel memory and works well only when the hits are sufficiently apart. In [12], various detectors for hit detection like locally most powerful (LMP), generalized likelihood ratio test (GLRT) and Bayes detector are presented. These detectors also ignore the system memory and perform detection of single hits. Subsequently a majority type rule is used for bit detection. The continuous time innovation $(e(t))$ is sampled at very high sampling rate $1/T_s$ such that $T_s << T_c$. As the channel response $(\Gamma(t))$ is finite length, the sampled channel response is assumed to have the finite length equal to M. The sampled channel response is given by,

$$\Gamma_0 = [\Gamma(t)|_{t=0} \ \Gamma(t)|_{t=T_s} \dots \ \Gamma(t)|_{t=(M-1)T_s}]^T$$

Determining when the cantilever is "hitting" the media and when it is not, is formulated as a binary hypothesis testing problem with the following hypotheses,

$$H_0 : \bar{e} = \bar{n}, \quad H_1 : \bar{e} = \Gamma_0 \nu + \bar{n}$$

where the sampled innovation vector $\bar{e} = [e_1 \ e_2 \dots e_M]^T$, $\bar{n} = [n_1 \ n_2 \dots n_M]^T$, Γ_0 is the sampled channel response, ν signifies the value of the impact on media and $VI_{M\times M}$ denotes the covariance matrix of $\bar{n}$ where $I_{M\times M}$ stands for $M \times M$ identity matrix. In case of locally most powerful (LMP) test given in [16], the likelihood ratio is given by [12],

$$l_{lmp}(M) \quad = \quad \frac{\partial}{\partial \nu} (\log \frac{f(\bar{e}|H_1)}{f(\bar{e}|H_0)})|_{\nu=0} = \bar{e}^T V^{-1} \Gamma_0.$$

where l_{lmp} denotes likelihood ratio for LMP. In our model, there are q number of hits in one bit duration. Let $l_{k,lmp}$ be the likelihood ratio corresponding to k^{th} hit. The decision rule for the detection of one bit in this case is defined as,

$$Max\Big(l_{1,lmp}(M) \ , l_{2,lmp}(M) \dots l_{q,lmp}(M)\Big) \lessgtr_1^0 \tau_1 \quad (15)$$

where τ_1 is LMP threshold. The likelihood ratio in the case of GLRT is [12],

$$l_{glrt}(M) \quad = \quad \log \frac{f(\bar{e}|H_1, \nu = \tilde{\nu})}{f(\bar{e}|H_0)} = l^2_{lmp},$$

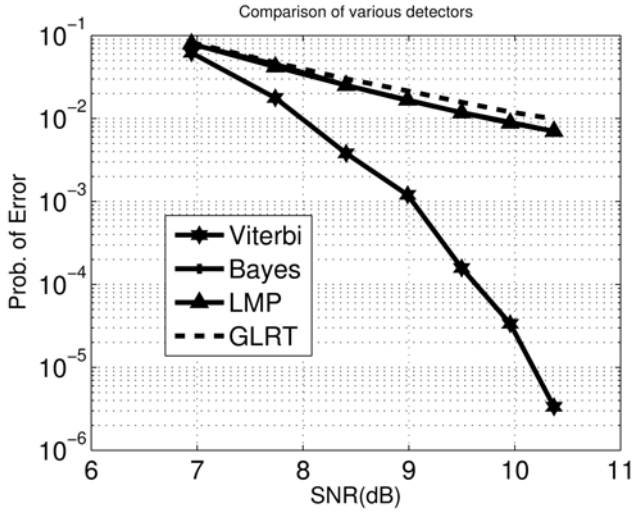

Fig. 6. Comparison of various detectors for simulation data. The Bayes curve is not visible in the graph as it coincides with the LMP curve.

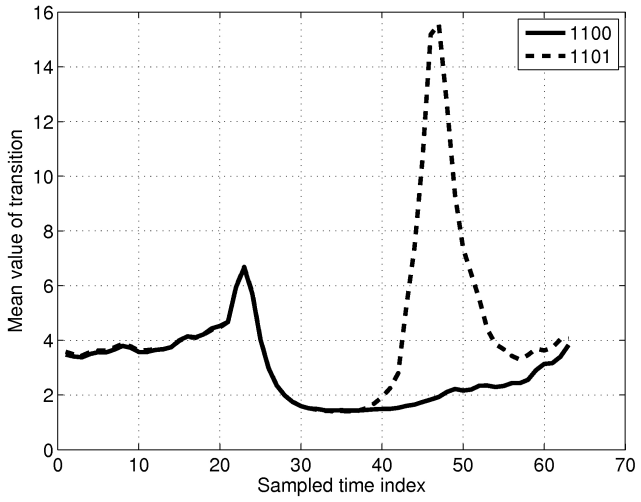

Fig. 7. Mean vector for 2 state transitions for 300 μs bit width from experimental data where '1100' and '1101' represents transition from state '110' to state '100' and '101' respectively.

where $\tilde{\nu}$ is maximum likelihood (ML) estimate of ν i.e. $\tilde{\nu} = \arg\max_{\nu} f(\bar{e}|H_1)$, l_{lmp} and l_{glrt} are likelihood ratios for LMP and GLRT case respectively. The decision rule for the bit detection in this case is defined in a similar manner given in (15).

Simulations from a Simulink model of the system can be run for a large number of hits in order to gather statistics on the discretized output of nonlinearity block which models the tip-media force. We modeled the statistics for ν by a Gaussian pdf with the appropriate mean and variance. With known mean and variance of ν the likelihood ratio for Bayes test is [12],

$$l_{bayes}(M) = \log \frac{f(\bar{e}|H_1)}{f(\bar{e}|H_0)} = \bar{e}^T V^{-1} \mu' + \frac{1}{2} \bar{e}^T V' \bar{e} - \bar{e}^T V' \mu',$$

where $\mu' = \Gamma_0 \alpha$ and $V' = \frac{\Gamma_0 \Gamma_0^T}{(\frac{V^2}{\lambda^2} + V \Gamma_0^T \Gamma_0)}$ and $\nu \sim N(\alpha, \lambda^2)$. The decision rule in this case is also defined in a similar manner given in (15). Note that ν is a measure of the tip-medium interaction force and as such it is difficult to experimentally verify the value of this force accurately which means the Bayes test cannot be applied for the bit detection on actual experimental data.

IV. Simulation Results

We performed simulations with the following parameters. The first resonant frequency of the cantilever f_0 = 63.15 KHz, quality factor Q =206, the value of forcing amplitude equal to 24 nm, tip-media separation is 28 nm, the number of hits in high bit duration is equal to 13 i.e. $q = 13$, discretized thermal and measurement noise variance are 0.1 and 0.001 respectively. A Kalman observer was designed and the length of the channel impulse response (I) was approximately 24 which means that m_I is equal to 2. We set the value of the system memory, $m = 1$. Using a higher value of m results in a more complex detector. We used a topographic profile where high and low regions denote bits '1' and '0' respectively and the bit sequence is generated randomly. The simulation was performed with the above parameters using the Simulink model that mimics the experimental station that provides a qualitative as well as a quantitative match to the experimental data. Tip-media interaction was varied by changing the height of media corresponding to bit '1'. We define the system SNR as the nominal tip-media interaction (nm) divided by total noise variance.

In Figure 6, we compare the results of four different detectors. The LMP, GLRT and Bayes detector perform hit detection, as against bit detection. In these detectors, the system memory is not taken into account. It is clear that the minimum probability of error for all detectors decreases as the tip-media interaction increases which makes SNR higher. The intuition behind this result is that hits become harder on media if tip-media interaction is increased which makes detection easier. The Viterbi detector gives best performance among all detectors because it incorporates the Markovian property of ν in the metric used for detection. At an SNR of 10.4 dB the Viterbi detector has a BER of 3×10^{-6} as against the LMP detector that has 7×10^{-3}.

V. Experimental Results

In experiments, a cantilever with resonant frequency $f_0 = 71.78$ KHz and quality factor $Q = 67.55$ is oscillated near its resonant frequency. A freshly cleaved mica sheet is placed on top of a high bandwidth piezo. This piezo can position the media (mica sheet) in z-direction with respect to cantilever tip. A random sequence of bits is generated through an FPGA board and applied to the z-piezo. High level is equivalent to 1 V and represents bit '1' and low level is 0 V and represents bit '0' thus creating a pseudo media profile of 6 nm height. The bit width can be changed using FPGA controller from $60 - 350\ \mu s$. The tip is engaged with the media at a single point and its instantaneous amplitude in response to its interaction with z piezo is monitored. The controller gain is kept sufficiently low such that the operation is effectively in open loop. The gain is sufficient to cancel piezo drift and maintain a certain level of tip-media interaction. An observer is implemented in another FPGA board which is based on the cantilever's free air model and takes dither and deflection signals as its input

and provides innovation signal at the output. The innovation signal is used to detect bits by comparing various bit detection algorithms. The experiments were performed on Multimode AFM, from Veeco Instruments. Considering a bit width of 40 nm and scan time of 60 μs gives a tip velocity equal to $2/3 \times 10^{-3}$ m/sec. The total scan size of the media is 100 micron which means the cantilever will take 0.15 seconds to complete one full scan. Read scan speed for this operation is 6.66 Hz. The read scan speed for different bit widths can be found in a similar manner.

The cantilever model is identified using the frequency sweep method wherein excitation frequency ω of $g(t) = A_0 \sin \omega t$ of dither piezo is varied from $0 - 100$ KHz and $p(t)$ is recorded. Magnitude and phase information about $G(i\omega)$ is obtained by evaluating the ratios between steady state amplitude and phase of output vs input excitation respectively. A second order transfer function is obtained that best fits the experimentally identified magnitude and phase responses of the cantilever. A, B and C matrices are obtained from the state space realization of the identified second order transfer function. F, G and H can be further found using the zero order hold discretization at a desired sampling frequency. The discretized state space of the cantilever model is used to find the discretized channel impulse response $\Gamma_{k;\theta}$ (see (3)).

For 300 μs bit width, there are around 21 hits in high bit duration and Viterbi decoding is applied on the innovation signal obtained from experiment. For experimental model, I is approximately 24 which means m_I is equal to 2. It is hard to estimate the system memory (m) from experimental parameters. Fortunately, there is a way around for this. As shown in the derivation of the detector, by making appropriate approximations, the final detector only requires the mean and the covariance of each branch in the trellis. These can be found by using training data and assuming various values of m. We have varied m from 0 to 2 and found the corresponding BER using these values of m. The total number of states in the Viterbi detector is 2^{m+m_I}. We have observed that for $m > 1$, the improvement in BER is quite marginal as compared to the increased complexity of Viterbi decoding. Accordingly we are using $m = 1$ for which the BER from Viterbi decoding is equal to 1×10^{-5} whereas the BER from LMP test is 0.26. The BER in the case of Viterbi decoding is significantly smaller when compared to the BER for usual thresholding detectors. If the bit width is decreased to 60 μs which means there are around 4 hits in the high bit duration, the BER for Viterbi decoding is 7.56×10^{-2} whereas the BER for LMP is 0.49 which means that LMP is doing almost no bit detection. As the bit width is decreased, there is more ISI between adjacent bits which increases the BER. The BER for different bit widths from all the detectors is shown in Figure 8. It can be clearly seen that Viterbi decoding gives remarkable results on experimental data as compared to the LMP detector. The Viterbi detector exploits the cantilever dynamics by modeling the mean and covariance matrix for different state transitions. We have plotted the mean vectors for 2 state transitions with 300 μs bit width in Figure 7. There are around 21 hits in one bit duration. The Viterbi decoding contains 8 states and 16 possible state transitions. In Figure 7, there is a clear distinction in mean vectors for different transitions which makes the Viterbi detector quite robust. Thresholding detectors like LMP and GLRT perform very badly on experimental data. For a bit sequence like '000011111', the cantilever gets enough time to go into steady state in the beginning and hits quite hard on media when bit '1' appears after a long sequence of '0' bits. The likelihood ratio for LMP and GLRT rises significantly for such high bits which can be easily detected through thresholding. However, a sequence of continuous '1' bits keeps the cantilever in steady state with the cantilever hitting the media mildly which means the likelihood ratio remains small for these bits. Thus it is very likely that long sequence of '1' bits will not get detected by threshold detectors.

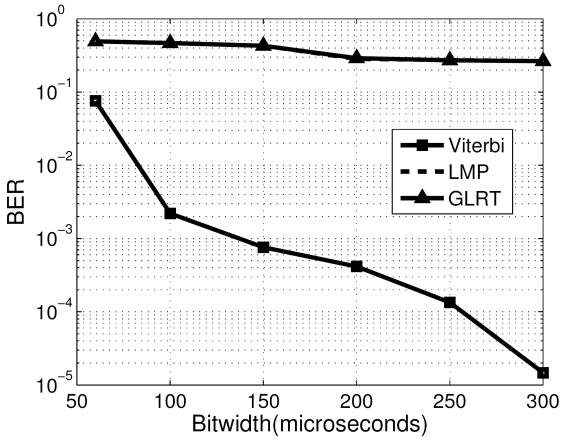

Fig. 8. BER for Viterbi, LMP and GLRT for different bit widths varying from 60 μs to 300 μs for experimental data. There is a very marginal difference between LMP and GLRT curve which is not visible in the graph but LMP does perform better than GLRT.

VI. Conclusions and Future Work

We presented the dynamic mode operation of a cantilever probe with a high quality factor and demonstrated its applicability to a high-density probe storage system. The system is modeled as a communication system by modeling the cantilever interaction with media. The bit detection problem is solved by posing it as a maximum likelihood sequence detection followed by Viterbi decoding. The main requirements for the proposed algorithm are (a) the availability of training sequences which can provide the statistics for different state transitions, (b) differences between the tip-media interaction magnitude between '0' and '1' bit and (c) an accurate characterization of the linear model of the cantilever in free air. Simulation and experimental results show that the Viterbi detector outperforms LMP, GLRT and Bayes detector and gives remarkably low BER. The work reported in this article demonstrates that competitive metrics can be achieved and enables probe based high density data storage, where high quality factor probes can be used in the dynamic mode operation. Thus, it alleviates the issues of media and tip wear in probe based high density data storage.

An efficient error control coding system is a must for any data storage system since the sector error rate specifications are on the order of 10^{-10} for systems in daily use such as hard drives. In future work, we are expecting to achieve this BER by

using appropriate coding techniques. Using run-length-limited (RLL) codes in our system is likely to improve performance and we shall examine this issue in future work. We are also working on a BCJR version of the algorithm to minimize the BER of the system even further. In experimental data, a small amount of jitter is inevitably present which is well handled by our algorithm. At high densities, the jitter will be significantly higher and we will need to apply more advanced modeling and detection techniques. These are part of ongoing and future work.

REFERENCES

[1] K. Aleksandar and J. M. F. Moura, "The Viterbi algorithm and Markov noise memory," *IEEE Trans. Inf. Theory*, vol. 46, no. 1, pp. 291-301, 2000.

[2] G. Casella and R. Berger, *Statistical Inference*. Duxbury Thomson Learning, 2nd edition, 2002.

[3] B. W. Chui, H. J. Mamin, B. D. Terris, D. Rugar, and T. W. Kenny, "Sidewall-implanted dual-axis piezoresistive cantilever for AFM data storage readback and tracking," in *Proc. Eleventh Annual International Workshop Micro Electro Mechanical Systems (MEMS'98*, pp. 12-17, Jan. 1998.

[4] R. D. Cideciyan, F. Dolivo, R. Hermann, W. Hirt, and W. Schott, "A PRML system for digital magnetic recording," *IEEE J. Sel. Areas Commun.*, vol. 10, no. 1, pp. 38-56, Jan. 1992.

[5] P. Baechtold, A. Sebastian, H. Pozidis, D. R. Sahoo, W. Haeberle, and E. Eleftheriou, "On intermittent-contact mode sensing using electrostatically-actuated micro-cantilevers with integrated thermal sensors," in *Proc. American Control Conf.*, pp. 2034-2039, June 2008.

[6] D. L. DeVoe and A. P. Pisano, "Modeling and optimal design of piezoelectric cantilever microactuators," *J. Microelectromechanical Syst.*, vo. 6, no. 3, pp. 266-270, Sep. 1997.

[7] U. Dürig, "Fundamentals of micromechanical thermoelectric sensors," *J. Applied Physics*, vol. 98, no. 44, 2005.

[8] E. Eleftheriou, T. Antonakopoulos, G. K. Binnig, G. Cherubini, M. Despont, A. Dholakia, U. Durig, M. A. Lantz, H. Pozidis, H. E. Rothuizen, and P. Vettiger, "Millipede: a MEMS-based scanning-probe data-storage system," *IEEE Trans. Magnetics*, vol. 39, no. 2, pp. 938-945, Mar 2003.

[9] E. Eleftheriou *et al*., "A nanotechnology-based approach to data storage," in *Proc. 29th International Conf. Very Large Data Bases (VLDB'2003)*, pp. 3-7, 2003.

[10] G. Forney, Jr., "Maximum-likelihood sequence estimation of digital sequences in the presence of intersymbol interference," *IEEE Trans. Inf. Theory*, vol. 18, no. 3, pp. 363-378, 1972.

[11] T. Kailath, A. H. Sayed, and B. Hassibi, *Linear Estimation*. Prentice Hall, 2000.

[12] N. Kumar, P. Agarwal, A. Ramamoorthy, and M. Salapaka, "Channel modeling and detector design for dynamic mode high density probe storage," in *Proc. 42nd Conf. Inf. Sciences Syst.*, 2008.

[13] J. Moon, "The role of SP in data-storage systems," *IEEE Signal Process. Mag.*, vol. 15, no. 4, pp. 54-72, July 1998.

[14] J. Moon and L. R. Carley, "Performance comparison of detection methods in magnetic recording," *IEEE Trans. Magnetics*, vol. 26, no. 6, pp. 3155-3172, Nov. 1990.

[15] J. Moon and J. Park, "Pattern-dependent noise prediction in signal-dependent noise," *IEEE J. Sel. Areas Commun.*, vol. 19, no. 4, pp. 730-743, Apr. 2001.

[16] H. V. Poor, *An Introduction to Signal Detection and Estimation*, 2nd edition. Springer-Verlag, 1994.

[17] D. R. Sahoo, A. Sebastian, and M. V. Salapaka, "Harnessing the transient signals in atomic force microscopy," *International J. Robust Nonlinear Control*, vol. 15, pp. 805-820, 2005.

[18] M. V. Salapaka, H. S. Bergh, J. Lai, A. Majumdar, and E. McFarland, "Multi-mode noise analysis of cantilevers for scanning probe microscopy," *J. Applied Physics*, vol. 81, no. 6, pp. 2480-2487, Mar. 1997.

[19] A. Sebastian, M. V. Salapaka, D. Chen, and J. P. Cleveland, "Harmonic and power balance tools for tapping-mode atomic force microscope," *J. Applied Physics*, vol. 89, no. 11, pp. 6473-6480, June 2001.

[20] R. D. Shachter, "Bayes-Ball: the rational pastime for determining irrelevance and requisite information in belief networks and influence diagrams," in *Proc. 14th Conf. Uncertainty Artificial Intelligence*, pp. 480-487, 1998.

[21] H. Thapar and A. Patel, "A class of partial response systems for increasing storage density in magnetic recording," *IEEE Trans. Magnetics*, vol. 23, no. 5, pp. 3666-3668, Sep. 1987.

[22] P. Vettiger, G. Cross, M. Despont, U. Drechsler, U. D¨urig, B. Gotsmann, W. H¨aberele, M. A. Lantz, H. Rothuizen, R. Stutz, and G. Binnig, "The "millipede"-nanotechnology entering data storage," *IEEE Trans. Nanotechnology*, vol. 1, no. 1, 2002.

[23] R. Wisendanger, *Scanning Probe Microscopy and Spectroscopy*. Cambridge University Press, 1994.

[24] R. Wood and D. Petersen, "Viterbi detection of class IV partial response on a magnetic recording channel," *IEEE Trans. Commun.*, vol. 34, no. 5, pp. 454-461, May 1986.

[25] Q. Zhong, D. Inniss, K. Kjoller, and V. B. Elings, "Fractured polymer/silica fiber surface studied by tapping mode atomic force microscopy," *Surface Science Lett.*, vol. 290, pp. L688-L692, 1993.

Naveen Kumar is a Ph.D. student in the department of Electrical and Computer Engineering at Iowa State University. He received his Masters Degree in Information and Communication Technology and Bachelors Degree in Electrical Engineering respectively in May 2005 at Indian Institute of Technology Delhi. His research areas include channel modeling, detector design and error control coding for dynamic mode high density probe storage, application of detection algorithms in Nano-imaging problems, multiuser scheduling and resource allocation.

Pranav Agarwal received B.Tech. degree in electrical engineering from Indian Institute of Technology, Kanpur, in 2000 and M.S. degree in electrical engineering from Iowa State University in 2007. He worked as design engineer at ST Microelectronics till 2004 where he was involved in digital design of sigma delta data convertors. He is currently a Ph.D. candidate at University of Minnesota, Twin Cities. His research interests include developing high bandwidth techniques for material characterization at nanoscale, quantitative imaging and signal processing algorithms involving probe based sensors and study of dynamics and control of processes at nanoscale.

Aditya Ramamoorthy received his B. Tech. degree in Electrical Engineering from the Indian Institute of Technology, Delhi in 1999 and the M.S. and Ph.D. degrees from the University of California, Los Angeles (UCLA) in 2002 and 2005 respectively. He was a systems engineer at Biomorphic VLSI Inc. till 2001. From 2005 to 2006 he was with the data storage signal processing group at Marvell Semiconductor Inc. Since Fall 2006 he has been an assistant professor in the ECE department at Iowa State University. He has interned at Microsoft Research in summer 2004 and has visited the ECE department at Georgia Tech, Atlanta in Spring 2005. His research interests are in the areas of network information theory, channel coding and signal processing for storage devices and its applications to nanotechnology.

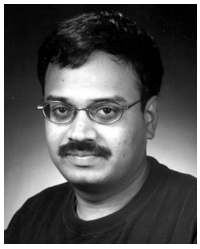

Murti Salapaka received the B.Tech. degree in mechanical engineering from Indian Institute of Technology, Madras, in 1991 and the M.S. and Ph.D. degrees in mechanical engineering from the University of California at Santa Barbara, in 1993 and 1997, respectively. He was a faculty member in the Electrical and Computer Engineering Department at Iowa State University from 1997 to 2007. Currently, he is a faculty member in the Electrical and Computer Engineering Department at the University of Minnesota, Minneapolis. His research interests are nanotechnology, multiple-objective robust control, and distributed and structural control. He is a 1997 National Science Foundation CAREER award recipient.